

# OPTIMUM SAMPLING FOR DIGITAL TERRAIN MODELLING

M. Charif

ITC, Department of Geoinformatics, P.O. Box 6, Enschede, The Netherlands, ISPRS Commission III

## ABSTRACT:

The investigation addresses three main issues: The first concerns a study of the terrain relief classification for the purpose of composite sampling. The second issue concerns quality assessment models that are used to assess the quality of representation of ideal geometric primitives and of real terrain relief representation. The third issue concerns the performance of composite sampling when applied to real terrain relief. In order to test the rules drawn from idealised geometric primitives on real terrain relief, two different terrain models were selected. First the skeleton information was sampled selectively, then Composite sampling was carried out. Finally, the quality was assessed implementing the quality assessment model. The analysis of the test results provides a feedback for optimizing the procedure for Composite Sampling.

**KEY WORDS:** Selective sampling, progressive sampling, skeleton information, filling information, composed transfer function, break line, peripheral line, rule base.

## INTRODUCTION

Digital Terrain Model (DTM) is a digital representation of the terrain relief serving for various purposes such as automatic contour plotting, digital orthophoto production, calculation of earth-work volumes etc.

Terrain relief modelling is the process of extraction and sampling of the spatial location of points or lines on terrain surface.

### 1. OPTIMUM SAMPLING

For large scale (detailed) DTM, optimum sampling can be a combination of semi-automatic progressive sampling (PS) of more homogeneous ( $\Pi$ -set) supplemented with manually controlled selective sampling (SS) of the skeleton information ( $\Sigma$ -set).

CS combines selective sampling ( $\Sigma$ -set) with progressive sampling ( $\Pi$ -set). The aim is to portray terrain relief faithfully without excessive redundancy of the sampled information.

The input consists of photographs of the terrain and the corresponding control data. The specified DTM grid is partitioned into square patches which act as the working units.

The output of CS is an incomplete regular DTM grid with density adapted to local terrain roughness, supplemented with the skeleton information ( $\Sigma$ -set). The original selectively sampled  $\Sigma$ -set is preserved in the data base.

To attain an optimal procedure the basic functions should be logically structured and adapted into the system component.

The four main stages of optimum sampling are shown in figure 1.

#### 1.1 Selective sampling

##### General.

SS is carried out manually to portray and /or isolate or exclude the anomalous regions in terrain. It is applied to abrupt changes in terrain slope, peripheries of water surfaces, clouds and image areas, with a poor stereoscopic hold, etc. Basically, SS is a subjective method of portraying the skeleton of terrain relief and of isolating the anomalous regions.

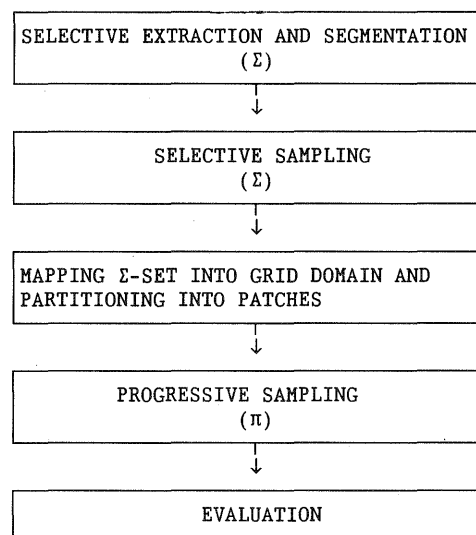


Fig. 1: Main stages of optimum sampling

#### 1.1.1 Selective sampling of anomalous regions.

General procedure for data preparation and feature extraction for Selective Sampling of distinct morphometric features and "anomalous terrain" ( $\Sigma$ -information), for the purpose of subsequent PS, is treated in (Makarovic, 1976)

Because SS is subjective, it needs to be systematised. To attain a balance between SS and PS and a smooth operation, some rules have been formulated. These represent the RULE BASE for SS and CS.

1.1.2 Rules for selective sampling. From the results of the experimental tests applied to ideal geometric generated primitives, their composite surface and to real terrain relief, the following rules have been extracted for selective sampling (as integral part of composite sampling):

The general procedure for segmentation, extraction and selective sampling of the terrain relief features, inside anomalous regions, are explained in (Charif, M. 1991). The corresponding rules for selective sampling of the terrain relief features are as follows:

Features approximating the geometric primitives are sampled only up to the following limits:

TERRAIN FEATURE	IF $H \geq \max$ and $Th/H \geq \max$	Then	Else
SPHERICAL SURFACE	2.0 % Z	1/10	S N
ELLIPSOIDAL SURFACE	1.5 % Z	1/7	S N
GAUSSIAN SURFACE	2.0 % Z	1/5	S N
CONICAL SURFACE	2.4 % Z	1/12	S N
COMPOSITE SURFACE	0.5 % Z	1/30	S N
HYPERBOLIC PARABOLOIDAL SURFACE	6.0 % Z	1/6	S N
BREAK LINE	2.0 % Z	1/8	S N
FAULT	2.0 % Z	1/3	S N

Table 1: Rules for selective sampling

Where

S= sample peak or pit (convex or concave) points and auxiliary lines,  
N= no SS and proceed to next working unit.

In the absence of auxiliary lines, some pseudo lines are generated automatically in the system.

The output of SS represents the  $\Sigma$ -set, which comprises:

- . peripheral lines
- . break lines and break points
- . auxiliary lines and auxiliary points
- . some descriptors.

This information serves as the input for the subsequent PS.

## 1.2 Progressive sampling

1.2.1 General. PS is a semiautomatic method for sampling terrain regions, mainly homogeneous, though irregular terrain relief, thus providing the filling information. The density of the DTM grid is locally adapted to terrain roughness.

1.2.2 Different densification criteria. The core of PS are the criteria for local grid densification. Hence, these criteria and the corresponding decision rules are most significant.

In (Makarovic, 1973) a one dimensional (1D) Laplacian operator was used separately in the X and Y directions. The following criteria are potential alternatives:

- . 2D-Laplacian,
- . Extended 2D-Laplacian,
- . 1D-Laplacian in four directions,
- . Median height,
- . Fitted plane,
- . Second difference for a quadruple of points, separately in the X and Y directions.

1.2.3 Tests using ideal geometric primitives as input The aim of the tests was to gain insight for identifying the most feasible densification rules in PS. To this end, some representative geometrically ideal primitive surfaces were used as input.

For the study, the following densification criteria were used:

- . VARIANT-1, PS(1); using 1D-Laplacian algorithm separately in X and Y
- . VARIANT-2, PS(2); using 2D-Laplacian algorithm

- . VARIANT-3, PS(3); using extended 2D-Laplacian algorithm
- . VARIANT-4, PS(4); using 1D-Laplacian algorithm separately in four directions.

For the geometric primitives tested, "1D-Laplacian in four directions" proves to be a potential alternative criterion for the self-adaptive densification in progressive sampling.

1.2.4 Procedure for progressive sampling including skeleton information The zero samplingrun covers all points of the initial coarse grid (Makarovic, 1977), after each sampling run analysis is performed of the heights for each triplet of points in the X and Y directions of the DTM grid.

Inside a triplet J-P, J, J+P (or I-P, I, I+P) a search is made in each of the four half intervals for the presence of the s points ( $\Sigma$ -set mapped in the DTM grid); figure 2, from the midpoints towards the grid points J-P, J, J+P (P represent variable grid interval).

1.2.5 Rules for composite sampling. These rules pertain to each triplet of points in the X and Y directions of the DTM grid.

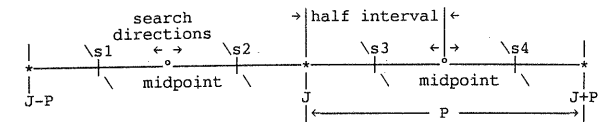


Fig. 2 Triplet of grid points with break points s

Based on the tests with the help of artificial ideal geometric primitives and their composite, a set of rules was extracted for optimum sampling, (Charif, M., 1991).

Despite the fact that the conclusions drawn from these tests are not generally representative, it is apparent that break lines, auxiliary lines and peripheral lines should be sampled to the extent mentioned in the rule base.

Distinct discrete points (peaks, pits, etc.) should be connected with the nearest lines rather than left isolated. The pseudo lines slightly improve CS, but generally do not replace the auxiliary lines.

To verify and consolidate the conclusions drawn from the experiments using artificial ideal geometric primitives and their composite, some experiments using real terrain relief are required.

Sampling real terrain relief feature, calls on the classification of terrain relief.

## 2. TERRAIN RELIEF ANALYSIS AND CLASSIFICATION

Terrain relief classification may serve for further studies in various earth sciences, agriculture, civil engineering, military activities, urban and rural surveying, residential and recreational planning and others.

In the context of optimum sampling for digital relief modelling, the purpose of classification is to provide some initial information on the terrain relief for specifying the sampling process. Thus, formulation of a suitable model for a quantitative terrain relief classification is necessary.

A terrain relief classification model should reflect the following requirements:

- . The classification should be simple, logical, and orderly.
- . The classification criteria should reflect the quality assessment model.
- . The classes should be distinct.
- . The classes should be finite and non-overlapping.
- . The classification should span the entire range of terrain relief characteristics.
- . The classification should be as objective as possible and based on quantifiable criteria.

### 2.1 Interrelationships.

An adequate classification model is a major prerequisite for the choice of the sampling procedure, such as to achieve a desired quality of DTM. Hence, there is strong interrelationship between the classification model, the quality assessment model, and the sampling procedure (figure 3).

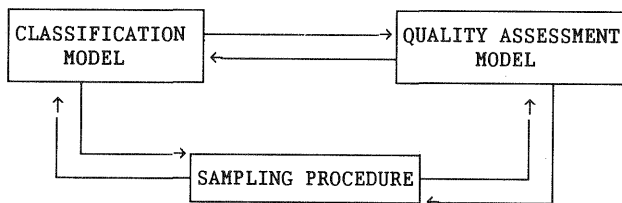


Fig. 3 Interrelationship between the classification model, the quality assessment model, and the sampling procedures

A given classification scheme affects both the quality assessment model and the sampling procedure. This is due to the fact that the different terrain classes may call for different sampling procedures. Moreover, classification scheme can be reflected on quality assessment models i.e., the quantified parameter values are used as input in accuracy assessment, for example if Transfer Function is used, then classification should be based on Fourier Transform or power spectrum.

A given quality assessment model influences the classification model and the sampling procedure. This is because a quality assessment model can be different for contour lines, profiles regular grids, etc..., these, however, require different sampling procedures.

Moreover, a given sampling procedure affects the classification scheme and the quality assessment model, because different sampling procedures result in different types of relief representation, and thus require different quality assessment models.

Therefore, the optimization implies mutual adjustment of these three models.

### 2.2 Approaches to terrain relief classification.

The terrain relief can be classified using different approaches, namely:

- . Qualitative approach
- . Quantitative approach
- . Mixed approach

Qualitative approaches are based on visual inspection of the information sources (maps, photographs, or of the terrain itself) (Way, 1978).

The qualitative approaches do not make use of any quantitative parameters, they are considered to be subjective approaches, therefore they will not be considered further.

Quantitative approaches use different quantifiable parameters of terrain relief such as Fourier transform, second difference, slope distribution, etc... These parameters, however, can be either deterministic or stochastic descriptors for relief, or a combination thereof.

Mixed approaches use combinations of qualitative and quantitative approaches.

In the following, some quantitative parameters for terrain relief classification are identified, after which a terrain relief classification model for the purpose of optimum sampling is devised.

### 2.3 Review of quantitative approaches.

In order to have an objective approach, the use of some quantifiable parameters describing the terrain relief becomes apparent. The application of most of these approaches, however, is limited due to the simplified assumptions on terrain relief.

Some typical examples of the quantifiable parameters are:

- a. Fourier transform or power spectrum
- b. distribution of the second difference (Laplacian)
- c. Ratio of the relief distance versus horizontal distance
- d. Slope distribution
- e. Direction cosine and eigenvectors
- f. Semi-variogram, auto-correlation or auto-covariance
- g. Fractal dimension
- h. Number and length of the break lines

The application of the criteria mentioned above is limited, due to the fact that the sampled profile is not representative of the whole area. The application of Fractal dimension, however, is limited due to some simplifying stochastic assumptions on terrain relief, such as self-similarity, stationarity, homogeneity, and isotropy.

The advantage of applying second difference criterion, ratio criterion, or semi-variogram criterion, however, is the simplicity in the computation. Moreover, the ratio criterion has a simple classification model, while the interpretation of the curve of semi-variogram is very simple.

In the following a method of classification for the purpose of optimum sampling, based on second difference criterion, will be presented.

### 2.4 CLASSIFICATION FOR THE PURPOSE OF OPTIMUM SAMPLING

The following example is suitable in the context of optimum sampling. The terrain relief information is differentiated according to the skeleton and filling sub-sets (Charif, M., 1991).

The skeleton information ( $\Sigma$ ) is represented by distinct lines and points, i.e., abrupt changes in relief. Break lines represent, mathematically, lines where the spatial derivatives are discontinuous. Physically they can pertain to natural features, or man made (natural) objects.

It is possible to extract the lines and points from a photogrammetric stereomodel, if they are distinct enough. The problem is to define an objective criterion for detecting break lines and points. In this context, however, a method based on the concept of profile analysis by applying the second difference criterion, is used.

The second difference in height of a triplet of points ( $\nabla^2h$ ) is compared with a certain preselected threshold value, in case ( $\nabla^2h$ ) is greater than the threshold, then the point belongs to the skeleton ( $\Sigma$ ), otherwise, as filling ( $\Pi$ ) information.

Hence the total terrain relief information (T) is composed of the skeleton ( $\Sigma$ ) and filling ( $\Pi$ )

$$T = \Sigma \cup \Pi \quad (1)$$

2.4.1 Classification of skeleton information for optimum sampling ( $\Sigma$ ) The skeleton  $\Sigma$  can be classified (Charif, 1991) according to the:

- Genetics

- . natural feature ( $\Sigma_N$ )
- . man-made objects ( $\Sigma_O$ )

$$\Sigma = \Sigma_N \wedge \Sigma_O \quad (2)$$

- Geometric entities:

- . Lines (L):
- . Distinct break-lines (BL): Ridge lines (DR), Drainage lines (DD), Convex (DV), Concave (DC)

$$BL = DR \wedge DD \wedge DV \wedge DC \quad (3)$$

- . Auxiliary (non distinct) lines (AL) Maxima (AX), Minima (AN), Others (AO)

$$AL = AX \wedge AN \wedge AO \quad (4)$$

- . peripheral lines (PL): Water (PW), Clouds (PC), other (PO)

$$PL = PW \wedge PC \wedge PO \quad (5)$$

Thus, all lines together:

$$L = BL \wedge AL \wedge PL \quad (6)$$

. Points (P):

- . Distinct break-points (BP): Peaks (DK), Pits (DT), Pass (DS), Convex (DE), Concave (DA)

$$BP = DK \wedge DT \wedge DS \wedge DE \wedge DA \quad (7)$$

- . Auxiliary (non distinct) points (AP): Peaks (AK), Pits (AT), Pass (AS), Convex (AE), Concave (AA)

$$AP = AK \wedge AT \wedge AS \wedge AE \wedge AA \quad (8)$$

Thus, all points together:

$$P = BP \wedge AP \quad (9)$$

Moreover the skeleton ( $\Sigma$ ) information can be differentiated further, according to the hierarchy of the information, to:

$$\Sigma = \Sigma_1 + \Sigma_2 + \Sigma_3 \quad (10)$$

where  $\Sigma_1$  is primary skeleton information,  $\Sigma_2$  is secondary skeleton information, etc ...

2.4.2 Classification of the filling information The filling information ( $\Pi$ ) represents the

terrain relief other than the skeleton  $\Sigma$ .  $\Pi$  is composed of incomplete regular grids of different densities.

The classification is inherent in the grids of the successive sampling runs:

$$\Pi = \Pi_0 + \Pi_1 + \Pi_2 + \Pi_3 + \Pi_4 \quad (11)$$

A possible quantitative criterion for classification is the relationship between ( $\Sigma$ ) and ( $\Pi$ ) information.

A) Natural terrain:

1. Smooth terrain, where  $\Sigma_{nat} \approx 0$

No of BL / unit area = 0.0

2. Slightly rough terrain, where  $\Sigma_{nat} \ll \Pi$

No of BL / unit area = 0.0 to 0.02

3. Moderately rough terrain, where  $\Sigma_{nat} < \Pi$

No of BL / unit area = 0.02 to 0.05

4. Very rough terrain, where  $\Sigma_{nat} \geq \Pi$

No of BL / unit area = 0.05 to 1.0

B) Urban, industrial, rural terrain:

1. Smooth terrain, where  $\Sigma_{art} \approx 0$

2. Slightly rough terrain, where  $\Sigma_{art} \ll \Pi$

3. Moderately rough terrain, where  $\Sigma_{art} < \Pi$

4. Very rough terrain, where  $\Sigma_{art} \geq \Pi$

Sampling real terrain feature should be assessed using some quality assessment measures, the latter needs to be studied in detail.

### 3. QUALITY MEASURES

DTM is meant for various applications, obviously the quality of DTM varies according to intended application. The quality of DTM intended for irrigation or large scale application would be different than that intended for small scale application. The objectives of this study are to define the quality assessment model for DTM, and study the relationship between the terrain classification, sampling procedure, and quality assessment.

The quality assessment of DTM is differentiated according to the performance (accuracy, fidelity), reliability, and efficiency (Charif, M., 1991).

#### 3.1 Performance

As it was stated earlier the performance is one of the main criteria influencing the estimation of the quality of DTM products. Performance was differentiated further according to completeness of  $\Sigma$  information, Accuracy of  $\Sigma$  and  $\Pi$  information, and the fidelity of  $\Sigma$  and  $\Pi$  information.

3.1.1 Accuracy In Composite Sampling, the terrain relief is represented by the  $\Sigma$  and  $\Pi$  sub-sets, consequently, the accuracy estimation should be differentiated according to;

- The standard error  $\sigma_{\Sigma}$  of modelling by the  $\Sigma$  set. This can be differentiated further according to

the  $\Sigma$ -subsets;

- . Discrete points, sampled stationary
- . Strings of points, sampled dynamically

- The standard error  $\sigma_{\Pi}$  of modelling by the  $\Pi$  set, which can be differentiated further according to the successive densification runs.

The standard error  $\sigma_{\Sigma}$  of modelling by the  $\Sigma$  set can be differentiated further according to accuracy, and comprehensiveness.

$$\sigma_{\Sigma} \begin{cases} \sigma_{\text{comprehensiveness}} (\sigma_c) \\ \sigma_{\text{accuracy}} (\sigma_a) \end{cases}$$

. Comprehensiveness  $\sigma_c$  of the  $\Sigma$ -set depends on the completeness of  $\Sigma$ -set (which features should be sampled and up to what extent), which depends on:

- . The criterion to detect non linearity in terrain relief
- . Threshold used in the criterion

. Accuracy  $\sigma_a$  of modelling by the  $\Sigma$ -set depends on:

- . Image quality and scale
- . Precision of instrument
- . Operator skill and care
- . Sampling mode (stationary, dynamically)

The standard error  $\sigma_{\Pi}$  of modelling by the  $\Sigma$ -set depends on:

- . Apriory  $\Sigma$ -set and  $\sigma_{\Sigma}$
- . Grid interval
- . Pointing error
- . Interpolation algorithm

Because the skeleton information is sampled prior to the filling information, it has an influence on the  $\Pi$ -set, thus  $\Sigma$ -set affects strongly the further modelling process.

### 3.2 Sources of errors

The accuracy of terrain relief modelling is influenced by two main sources of errors:

- . Error of sampling and interpolation  $\sigma_s$ , mentioned earlier
- . Measuring error  $\sigma_m$ , depending on; setting error, the quality of photography, type of terrain, model scale, precision of the instrument, and the skill and care of the operator.

Assuming  $f(x)$  is the terrain profile, and  $f_i(x)$  is the correct height of a point and  $g_i(x)$  is the sampled height:

$$g_i(x) = f_i(x) + m_i(x) \quad (12)$$

In photogrammetric measurement  $m_i(x)$  is considered partly systematic, and partly random, thus the latter part of  $m_i(x)$ , can be defined as a sequence of uncorrelated values, which are normally distributed, with the mean equal to zero and the variance  $\sigma_m^2$ .

Assuming that  $f_i(x)$  and  $m_i(x)$  are mutually independent and thus uncorrelated, the variance of the error of the modelling is:

$$\sigma_T^2 = \sigma_s^2 + \sigma_r^2 \quad (13)$$

where  $\sigma_s$  is the error of sampling and interpolation, and  $\sigma_r$  is caused by the  $\sigma_m$ .

In (Tempfli, 1986) it has been found that there is a simple relation;

$$\sigma_r^2 = 2/3 \Delta x^2 \sigma_m^2 \quad (14)$$

In the case of a regular grid and in the absence of measuring error, the error of sampling and interpolation can be defined as (Tempfli, 1986);

$$\sigma_s^2 = \sum_{k=-n/2}^{n/2-1} \{ 1 - H(vk) \}^2 \quad (15)$$

Where  $|F(k)|$  is the discrete amplitude spectrum of the input obtained by FFT.

### 3.3 Estimation of the sampling error $\sigma_s$

Accuracy of DTM can be estimated by analytical, semi analytical, or experimental approaches.

3.3.1 Analytical approach Terrain profile (surface) can be transformed into the frequency domain (Fourier Transform). The transfer Function of sampling and interpolation can be determined and used for quality assessment (Laan,1973).

Fidelity of the reconstruction (transfer ratio) can be computed for various sampling interval ( $\Delta x$ ), and plotted against different  $\Delta x$  (Makarovic, 1976).

Transfer Function can be used either for the planing purpose or for Accuracy estimation of DTM, reconstructed by sampling and interpolation.

The advantage of this approach is that there is no need for classification and also its simplicity in practical application, but the approach is conceptually involved.

3.3.2 Semi analytical approach Applying the law of error propagation, the error of the reconstruction  $\hat{H} - H \rightarrow \min$  can be computed (Kubik, K., 1986).

A low polynomial (trend) is substructured from the input (terrain surface) in order to create the stationarity condition, and  $\sigma_0$ , and the covariance are estimated (stochastic assumptions),  $\sigma_H$ ,  $\sigma_{\text{mean}}$ , and  $\sigma_{\text{max}}$  computed, for error estimation.

Shortcoming of the method is some simplified stochastic assumption on terrain surface (homogeneous, stationary, and isotropy) which can seldom be realised in case of real terrain relief.

3.3.3 Experimental approach Real terrain relief. The reconstructed surface of the real terrain relief is compared to the original surface and the fidelity of the reconstruction is estimated.

The flow diagram of the approach is shown in figure 4.

The advantage of this approach is that it is conceptually simple.

The shortcoming of the approach is that extensive experiments and terrain classification are required.

### 3.4 Fidelity of DTM obtained by PS

The fidelity of sampling and interpolation (in case of fixed  $\Delta X$ ) can be studied by its transfer function.

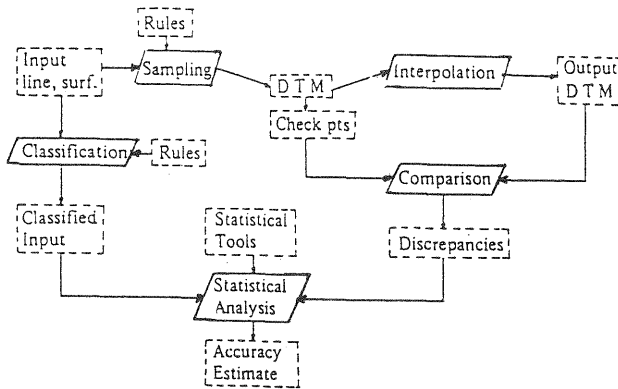


Figure 4: Experimental Approach to accuracy estimation of real terrain relief

Strictly speaking, in the case of irregularly spaced points, the application of a single transfer function to study the problem of fidelity in the Fourier transform is not possible.

In progressive sampling the point density is doubled in each run a composed transfer function can be constructed for PS (Tempfli, 1986) and used to assess the fidelity of DTM resulting from PS.

$$H(\nu, Th, r) = 1 - \sqrt{2} \sigma^2(\nu, Th, r) \quad (16)$$

This is a function composed of segments of the partial transfer functions, for incomplete regular grids of different densities corresponding to the successive sampling runs  $r$ , applied to sinusoids  $\sin(2\pi\nu\Delta X)$  with different frequencies  $\nu \in (0, 1/2)$ .

To this end a limiting fidelity function is introduced;

$$\Phi(\nu_k, Th) = \{P(\nu_k) - a \cdot Th\} / P(\nu_k) \quad (17)$$

Where  $a \cdot Th$  is the maximum error acceptable in progressive sampling and the factor "a" depends on the magnitude of the threshold and on the type of the input (Makarovic, B., 1976).

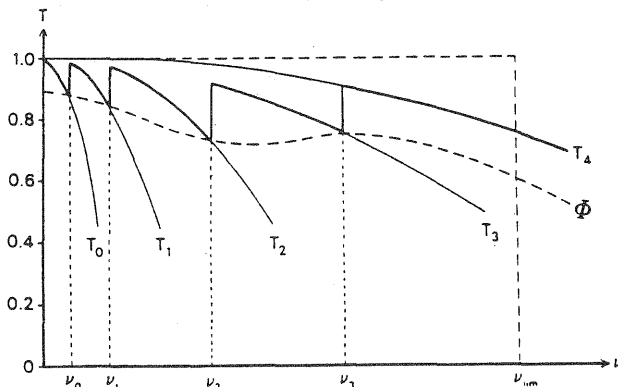


Figure 5: Composed transfer function

By considering criteria inherent in progressive sampling, the sections of Transfer Function (TF) below the  $\Phi$  curve should be rejected, and the composed TF used for the purpose of accuracy estimation.

Estimation of the accuracy as function of fidelity of PS can be approached from the viewpoint of the two extremes:

- . Lower bound accuracy ( $\sigma_{\min}$ )
- . Upper bound accuracy ( $\sigma_{\max}$ )

The lower bound accuracy ( $\sigma_{\min}$ ) of PS can be estimated by using the transfer function for the regular grid with  $\Delta X = \Delta r_{\max}$ , and discrete amplitude spectrum which is computed by FFT.

$$\sigma = \sum_{k=-n/2}^{n/2-1} \{1 - H(\nu_k, Th, r_{\max})\}^2 |F(k)|^2 \quad (18)$$

Where  $P(\nu_k) = 2|F(k)|$ ,  $|F(k)|$  = the discrete amplitude spectrum of the input obtained by FFT.

The upper bound accuracy ( $\sigma_{\max}$ ) of PS can be estimated by using the composed transfer function.

The actual accuracy of PS based on sampling and interpolation would be:

$$\sigma_{\min} \leq \sigma_{\text{actual}} \leq \sigma_{\max} \quad (19)$$

The estimation of the accuracy by means of the Transfer Function is possible only when the amplitude spectrum of the terrain is known. When terrain exhibits a predictable amplitude spectrum, an approximate estimation of the overall accuracy is possible.

Because investigations were performed with the help of some artificial ideal geometric primitives, where the input was precisely known as well as with real terrain relief, the experimental approach to accuracy estimation was obvious.

As it was stated earlier the overall standard error ( $\sigma_r$ ) of the reconstructed surface is not very suitable for the assessment of accuracy. In this investigation, however, the following additional measures are used for the quality assessment of DTM.

- . The efficiency of the surface modelling process, which is affected by factors such as distribution of the sampled points (points representing skeleton information and those representing the filling information), and the average number of the sampled points per unit area.
- . The maximum discrepancy between true and modelled height.
- . Reliability is quantified by the number of correct heights divided by the total number of heights.
- . Fidelity of the modelled relief can be defined by a transfer function, which describes the combined effects of sampling and interpolation (Makarovic, 1976).

### 3.5 Assessment criteria

Quality of the reconstruction is influenced by the following factors;

- . Amount of skeleton information ( $\Sigma$ )
- . Quality of skeleton information ( $\sigma_r$ )
- . Sampling interval for filling information ( $\Pi$ )
- . The value of threshold used for densification
- . Number of densification runs
- . Number of sampled points

### Real terrain relief

Quality of the reconstruction of the real terrain relief can be assessed using the following criteria:

- The mean error  $\sigma_{PS}$  of PS is determined for all

the grid points (sampled and interpolated) on the modelled surface of the patch.

$$\sigma_{PS} = \sqrt{(\Sigma v^2 / N_{\pi})} \quad (20)$$

Where  $v^2$  represent the discrepancy between true and modelled heights, and  $N_{\pi}$  is the number of points in the patch.

For comparison with other tests, the mean error is normalised with the maximum height in the patch  $H_{max}$ .

$$\sigma_{PS} = \sigma_{PS} / H_{max} \quad (21)$$

- The mean error  $\sigma_{CS}$  (of CS) for comparison with  $\sigma_{PS}$ , was estimated for the same number of points ( $N_{\pi}$ ) as used for  $\sigma_{PS}$ . Outside that area, there are no discrepancies. Thus

$$\sigma_{CS} = \sqrt{(\Sigma v^2 / N_{\pi})} \quad (22)$$

where  $v$  is the discrepancy between the modelled and the true height. The number of sampled points and the number of interpolated points are obviously not the same as in the case of PS, however the total number of the points is the same.

This mean error can also be normalised by  $H_{max}$ .

$$\bar{\sigma}_{CS} = \sigma_{CS} / H_{max} \quad (23)$$

- In each experiment the maximum discrepancy between the ideal and the interpolated DTM surface was normalised by  $H_{max}$ , i.e., to have a measure that is independent of the height of the primitive:

$$\overline{MAXER} = \text{maximum discrepancy} / H_{max} \quad (24)$$

- The sampling efficiency is defined by the number of sampled points per unit area:

$$\bar{E} = \frac{[\text{Numb of sampl. pts}]}{[\text{total Numb. of pts per grid}]} \quad (25)$$

For comparative assessment, the relative differences in performance and the ratios of the performances are suitable. This is because a relative difference is a measure of gain or loss, while a ratio is independent of the magnitude of the errors.

$$\Delta \sigma = \text{gain (+) or loss (-) in the mean error } \sigma, \quad (26)$$

Ratio of the mean error of PS and CS:

$$R_{\sigma_{CS/PS}} = \sigma_{PS} / \sigma_{CS} \quad (27)$$

Ratio of the mean error for CS3 and CS2:

$$R_{\sigma_{CS(3)/CS(2)}} = \sigma_{CS(2)} / \sigma_{CS(3)} \quad (28)$$

$$\Delta \text{ MAXER} : = \text{increase or decrease of the maximum error,} \quad (29)$$

Ratio of the maximum error of PS and CS:

$$R_{\text{MAXER}_{CS/PS}} = \text{MAXER}_{PS} / \text{MAXER}_{CS} \quad (30)$$

Ratio of maximum error of CS3 and CS2:

$$R_{\text{MAXER}_{CS(3)/CS(2)}} = \text{MAXER}_{CS(2)} / \text{MAXER}_{CS(3)} \quad (31)$$

$$\Delta E = \text{gain or loss in the efficiency} \quad (32)$$

Ratio of the efficiency of PS and CS:

$$R_{E_{CS/PS}} = R_{PS} / R_{CS} \quad (33)$$

Ratio of the efficiency of CS3 and CS2:

$$R_{E_{CS(3)/CS(2)}} = R_{CS(2)} / R_{CS(3)} \quad (34)$$

#### 4. OPTIMUM SAMPLING APPLIED TO REAL TERRAIN RELIEF

To verify and consolidate the conclusions drawn from the experiments using artificial ideal geometric primitives and their composite some experiments using real terrain relief as the input were conducted. A realistic S-factor is  $S=1/16$ .

##### 4.1 Experimental test

4.1.1 Haifa region Aerial photos were  $23 \times 23$  cm, Scale = 1:30,000,  $c = 150$  mm Camera type = Wild RC 10, the Easting of the area was between 145.000 and 147.000, the Northing between 220.000 and 225.000 The area selected for testing was composed of partly rough and partly smooth terrain, the altitude of terrain was between  $H_{max} = 164.992$  m and  $H_{min} = 9.708$  m. The flat part of the area was used for agricultural purpose, and the rest was covered partly by small trees and bushes, and partly by a few buildings. The instrument was KERN DSR-1 Analytical stereoplotter.

##### a. Selective sampling:

Two regions with some abrupt changes have been delimited from a more homogeneous terrain, with the break lines acting at the same time as the peripheral lines. These lines were sampled selectively, by using the MAPS 200 system E-set 1 (figure 8).

Inside these regions the break lines and break points which fulfil the specifications of the rule base were sampled selectively, by using MAPS 200 system, E-set 3 (figure 9).

All the break lines which fulfil the specifications of the rule base, except the break lines joining the peaks, were sampled selectively, by using MAPS 200 system, E-set 2 (figure 10).



Figure 8:  
E-set 1

Figure 9:  
E-set 2

Figure 10:  
E-set 3

a.1 Regular grid:

In order to use off-line Composite Sampling, terrain relief was represented by a dense regular grid, with a grid spacing of 25 m.

a.2 Sampled information:

The  $\Sigma$ -information contained 1601 points in vector form, sampled selectively, which are arranged in tree subsets, namely;

- $\Sigma$ -set 1
- $\Sigma$ -set 2
- $\Sigma$ -set 3

The terrain relief was represented by 16000 points which are arranged in a regular grid forming 250 (25\*10) patches of 8\*8 points each.

a.3 Preprocessing

a.3.1  $\Sigma$ -sets

$\Sigma$ -sets were mapped into the grid domain. The rasterised format  $\Sigma$ -sets were then segmented into 44 overlapping patches of 33\*33 points each.

a.3.2 Regular grid

The regular grid consisting of 250 patches (of 8\*8 points each) was segmented into 44 overlapping patches of 33\*33 points each.

b. Progressive and composite sampling, TEST 1 : PS

- Input:
- . Regular grid DTM consisting of 44 overlapping patches of 33\*33 points each.
- . Threshold (for second differences)  
Th = 10.0 m (S = 1/16)
- Maximum height difference  $\Delta H_{max}$  in the test area = 155.214 m

TEST CASE	S =	VARIANT	$\bar{\sigma}$	MAXER	E
TEST 1	1/16	PS	2.0 %	12.0 %	35 %

Table 2: Performance measures for PS

TEST 2 : VARIANT-1; CS(1)

Input:

- . Same as previous test + $\Sigma$ -set 1

TEST CASE	S =	VARIANT	$\bar{\sigma}$	MAXER	E
TEST 2	1/16	CS(1)	2.0 %	5.0 %	33 %

Table 3: Performance measures for CS(1)

TEST 3: VARIANT-2; CS(2)

Input:

- . Same as previous test + $\Sigma$ -set 2

TEST CASE	S =	VARIANT	$\bar{\sigma}$	MAXER	E
TEST 3	1/16	CS(2)	1.9 %	5.0 %	29 %

Table 4: Performance measures for CS(2)

TEST 4: VARIANT-3; CS(3)

Input:

- . Same as previous test + $\Sigma$ -set 3

TEST CASE	S =	VARIANT	$\bar{\sigma}$	MAXER	E
TEST 4	1/16	CS(3)	1.8 %	5.0 %	30 %

Table 5: Performance measures for CS(3)

c. Performance estimates for progressive and composite sampling

PATCH	VARIANT	$\sigma$	$\sigma$ % OF Z	MAXER	PS PTS	% PS PTS
1,1 to 11,4	CS(3)	0.82	1.8 %	8.30	3434	30 %
	CS(2)	0.86	1.9 %	8.30	3404	29 %
	CS(1)	0.89	2.0 %	8.30	3733	33 %
	PS	0.91	2.0 %	19.65	3997	35 %

Table 6: performance estimates for progressive and composite sampling

CS(3) =  $\Sigma$ -set contains all the break lines which fulfil the requirement of rule base.

CS(2) =  $\Sigma$ -set contains all the previous break lines, except the break lines joining the peaks.

CS(1) =  $\Sigma$ -set contains only Main break lines which are at the same time peripheral lines of anomalous regions.

In order to reflect the role of  $\Sigma$  information in the sampling, results of different tests were compared.

TEST	S	R $\sigma$	R max	R E
CS(3) versus PS	1/16	1.11	2.37	1.17
CS(2) versus PS	1/16	1.06	2.37	1.17
CS(1) versus PS	1/16	1.02	2.37	1.06

Table 7: Performance estimation of different variants of CS with respect to PS

In conclusion we can state, by using the break lines and break points which fulfil the specifications of the rule base in CS(3), that apart from a grate improvement in the accuracy of the skeleton information, the overall accuracy and overall efficiency are also improved significantly, compared to PS ( $R_{\sigma} = 11\%$  and  $R_E = 17\%$ ).

When omitting the peaks and the auxiliary lines joining these peaks, the gain in overall accuracy is reduced by 5% and overall efficiency did not changed (compared to CS(3)).

When omitting the break lines and break points which fulfil the specifications of the rule base, and by using only the main break lines, the gain in the overall accuracy is reduced by 9% and the gain in overall efficiency is improved by 11% (compared to CS(3)).



Fig. 10a: Contour map, Haifa

4.1.2 Bonnieux region This model is partly covered by flat, and partly by accidental terrain. This justifies perfectly the use of optimum sampling. Aerial photos were 23 \* 23 cm, Scale = 1/15.000, c = 150 mm Camera type = Wild RC 10, the

Easting of the area was between 840.200 and 841.800, the Northing between 174.000 and 176.880 the altitude of terrain was between  $H_{max} = 482.000$  m and  $H_{min} = 243.000$  m, the instrument was KERN DSR-1 Analytical stereoplottter.

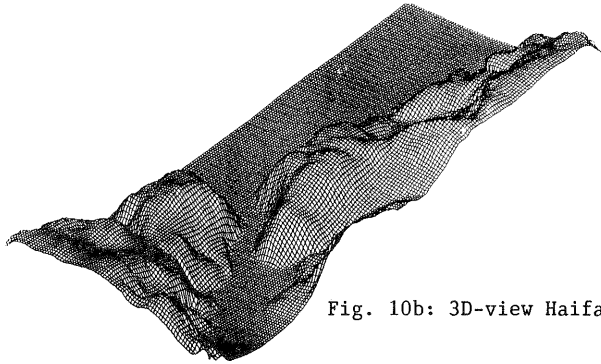


Fig. 10b: 3D-view Haifa

a. Selective sampling:

Two regions with some abrupt changes have been delimited from a more homogeneous terrain, with the break lines acting at the same time as the peripheral lines. These lines were sampled selectively, by using the MAPS 200 system. Moreover, inside these regions the break lines and break points which fulfil the specifications of the rule base were also sampled selectively,  $\epsilon$ -information (figure 11).



Fig. 11: Information  $\epsilon$  Bonnieux

a.1 Regular grid:

In order to use the off-line version of optimum sampling, terrain relief was represented by a dense regular grid of 20 m interval.

a.2 Sampled information:

The  $\epsilon$ -information contained 382 points in vector form, sampled selectively.

The terrain relief was represented by 16384 points which are arranged in a regular grid forming 128 (16\*8) patches of 8\*8 points each.

a.3 Preprocessing:

a.3.1  $\epsilon$ -information:  $\epsilon$ -sets were mapped into the grid domain and segmented into 44 overlapping patches of 33\*33 points each.

a.3.2 Regular grid: The regular grid consisting of

250 patches (of 8\*8 points each) was segmented into 44 overlapping patches of 33\*33 points each.

b. Progressive and composite sampling:

TEST 1:PS

Input:

- . Regular grid DTM consisting of 44 overlapping patches of 33\*33 points each.
- . Threshold (for second differences)  
Th = 5.0 m (S = 1/48)
- Maximum height difference  $\Delta H_{max}$  in the test area = 243.79 m

TEST CASE	S =	VARIANT	$\bar{\sigma}$	MAXER	E
TEST 1	1/48	PS	0.08 %	1.20 %	71 %

Table 8: Performance measures for PS

TEST 2: VARIANT-1; CS

Input:

- . Same as previous test +  $\epsilon$ -information

TEST CASE	S =	VARIANT	$\bar{\sigma}$	MAXER	E
TEST 2	1/48	CS	0.06 %	0.58 %	65 %

Table 9: Performance measures for CS

c. Performance estimates for progressive and composite sampling

PATCH	VARIANT	$\sigma$	$\sigma$ % OF Z	MAXER	PS PTS	% PS PTS
1,1 to 8,4	CS	0.31	0.6 %	2.78	5336	65 %
	PS	0.36	0.8 %	5.87	5842	71 %

Table 10: Performance estimates for progressive and composite sampling

CS =  $\epsilon$ -set contains all the break lines which fulfil the requirement of rule base.

In order to reflect the role of  $\epsilon$  information in the sampling, results of different tests were compared.

TEST	S	R $\sigma$	R max	R E
CS versus PS	1/48	1.33	2.11	1.10

Table 11: Performance estimation of different variants of CS with respect to PS

In conclusion we can state the following:

The fidelity of the representation is improved by using the break lines and break points. Apart from a great improvement in the accuracy of the skeleton information, the overall accuracy and overall efficiency are also improved significantly, compared to PS ( $R_g = 33\%$  and  $R_e = 10\%$ ). Finally, for this region, we observe that by using the break lines and break points which fulfil the specifications of the rule base we can get, not only a better representation, but also more accuracy, with less effort.

5. CONCLUSIONS

By including the  $\epsilon$  information (peripheral lines, break lines, peaks and pits) in the sampling

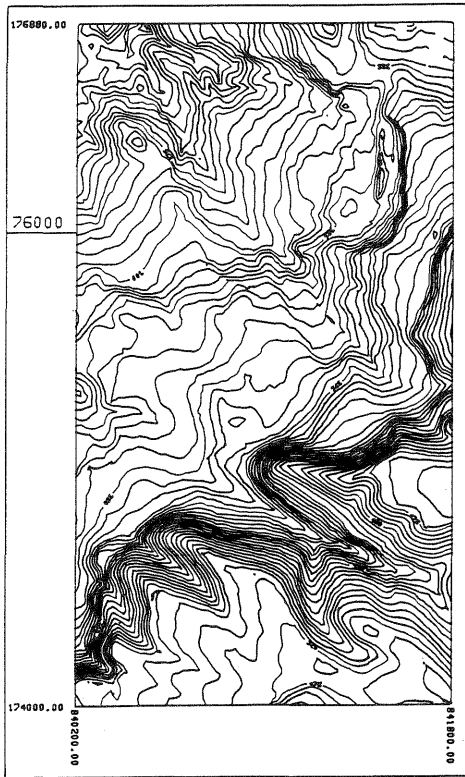


Fig. 12: Contour map, Bonnieux

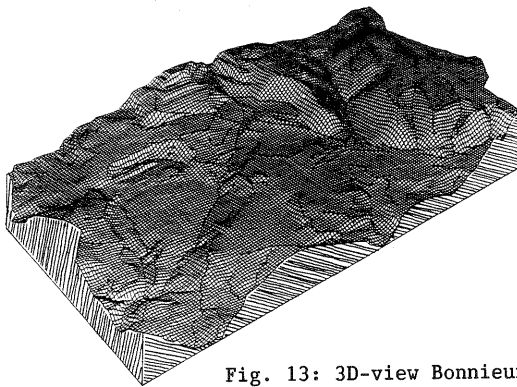


Fig. 13: 3D-view Bonnieux

procedure, the accuracy increases, when the threshold is selected properly. The gain in accuracy is highly correlated with the threshold value, increasing the value of threshold causes an increase in the gain of accuracy and vice versa. At the same time, inclusion of  $\epsilon$  information results a considerable gain in efficiency. we observe a negative correlation between the gain in the efficiency and the value of the threshold. The latter reduces as a result of increasing the value of the threshold.

From the results of the experiments of sampling applied to ideal geometric primitives, a simulated composite surface, and real terrain reliefs, certain additional rule bases were set up.

Rule base to systemize selective sampling, and rules for the procedure of sampling in the subsequent phase of progressive sampling, in order to achieve a balance between  $\epsilon$  and  $\Pi$  information, are reflecting an optimum sampling.

## REFERENCES

- Ayeni, O., 1976. Objective terrain description and classification. I.S.P.R.S. 23(III/1), pp 1-8.
- Charif, M., 1991. Echantillonnage optimal pour modele numerique de terrain, partie integrante d'un systeme d'information geographique. Ph.D.Thesis, Paris 7 University, France, 135 pp.
- Charif, M., Makarovic, B., 1988. Optimizing progressive and composite sampling for Digital Terrain Model, I.S.P.R.S.,27(B10): III-264-280, Kyoto
- Fredrikson, Poul., Jacobi, Ole., Kubik, K., 1983. Optimal sample spacing in Digital Terrain Models" I.S.P.R.S. Proceeding, commission 3.
- Fredrikson, Poul., Jacobi, Ole., Kubik, K., 1984. Accuracy prediction in Digital Elevation Models, I.S.P.R.S. Rio do Janeiro, 26 (3/1), pp. 246-255.
- Fredrikson, Poul., Jacobi, Ole., Kubik, K., 1984. Modelling and classifying terrain, I.S.P.R.S. Rio do Janeiro, pp. 256-265.
- Mandelbort, B.B., 1982. The fractal geometry of nature, W.H. Freeman and co. San Francisco, 480 pp.
- Kubik, K., Roy, B., 1986. Digital terrain model workshop proceedings. Columbus, Ohio, 150 pp.
- Laan, R.C., 1973. Information transfer in reconstruction of data from sampled points of a sinewave" I.T.C. Journal 1973, 3, pp 379-396.
- Makarovic, B., 1973. Progressive Sampling for DTM's, I.T.C. Journal 1973-3 pp 397-416.
- Makarovic, B., 1976. A Digital Terrain Model System, I.T.C. Journal 1976-1, pp 57-83.
- Makarovic, B., 1976. Conversion of fidelity into accuracy, I.T.C. Journal, pp 507-517.
- Makarovic, B., 1977. Composite Sampling for Digital Terrain Model I.T.C. Journal 1977-3, pp 406-431.
- Tempfli, K., 1986. accuracy of Digital Terrain Model obtained by Progressive Sampling, ITC publication, pp 10.
- Tempfli, K., 1980. Spectral analysis of terrain relief for the accuracy estimation of DTM, I.T.C. Journal 1980-3, pp 478-510.